Spectrochimica Acta Part A: Molecular and Biomolecular Spectroscopy 102 (2013) 226–234

Contents lists available at SciVerse ScienceDirect

Spectrochimica Acta Part A: Molecular and Biomolecular Spectroscopy

journal homepage: www.elsevier.com/locate/saa

Host–guest interaction between new nitrooxoisoaporphine and β-cyclodextrins: Synthesis, electrochemical, electron spin resonance and molecular modeling studies

Fernanda Pérez-Cruz [a], Benjamín Aguilera-Venegas [a,b], Michel Lapier [a], Eduardo Sobarzo-Sánchez [c], Eugenio Uriarte Villares [d], Claudio Olea-Azar [a,*]

[a] Department of Inorganic and Analytical Chemistry, Faculty of Chemical and Pharmaceutical Sciences, University of Chile, Sergio Livingstone 1007, Santiago, Chile
[b] Laboratory of Antioxidants, Institute of Nutrition and Food Technology, University of Chile, Av. Macul 5540, P.O. Box 138-11, Santiago, Chile
[c] Departamento de Farmacia y Tecnología Farmacéutica, Facultad de Farmacia, Universidad de Santiago de Compostela, 15782 Santiago de Compostela, Spain
[d] Departamento de Química Orgánica, Facultad de Farmacia, Universidad de Santiago de Compostela, 15782 Santiago de Compostela, Spain

HIGHLIGHTS

- A new nitrooxoisoaporphine derivative was synthesized.
- Electrochemical mechanisms were elucidated by cyclic voltammetry.
- Hyperfine splitting patterns were established by ESR spectroscopy.
- Nitrooxoisoaporphine-β-cyclodextrin inclusion complex was formed.
- Inclusion geometries were revealed by 2D-NMR and molecular modeling.

GRAPHICAL ABSTRACT

The inclusion complexes of new nitrooxoisoaporphine with β-cyclodextrin, hydroxypropyl-β-cyclodextrin and dimethyl-β-cyclodextrin, have been investigated using cyclic voltammetry, ^{1}H NMR, 2D NMR, ESR and molecular modeling studies.

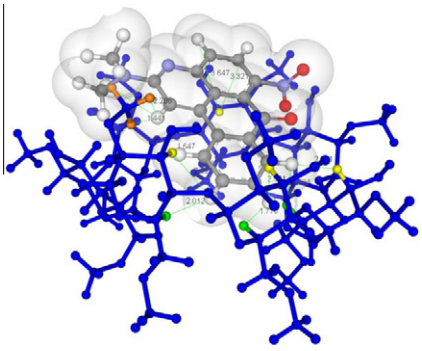

ARTICLE INFO

Article history:
Received 26 April 2012
Received in revised form 14 September 2012
Accepted 22 September 2012
Available online 26 October 2012

Keywords:
Nitrooxoisoaporphine
Cyclic voltammetry
ESR
Cyclodextrin complexes
Theoretical calculation
Molecular modeling

ABSTRACT

A new nitrooxoisoaporphine derivative was synthetized and characterized by cyclic voltammetry and electron spin resonance. Its aqueous solubility was improved by complexes formation with β-cyclodextrin, heptakis(2,6-di-O-methyl)-β-cyclodextrin and (2-hydroxypropyl)-β-cyclodextrin. In order to assess the inclusion degree reached by nitrooxoisoaporphine in cyclodextris cavity, the stability constants of formation of the complexes were determined by phase-solubility measurements obtaining in all cases a type-A_L diagram. Moreover, electrochemical studies were carried out, where the observed change in the EPC value indicated a lower feasibility of the nitro group reduction. Additionally, a detailed spatial configuration is proposed for inclusion of derivate within the cyclodextrins cavity by 2D NMR techniques. Finally, these results are further interpreted by means of molecular modeling studies. Thus, theoretical results are in complete agreement with the experimental data.

* Corresponding author. Tel.: +56 2 9782844; fax: +56 2 7370567.
E-mail address: colea@uchile.cl (C. Olea-Azar).

1386-1425/$ - see front matter © 2012 Elsevier B.V. All rights reserved.
http://dx.doi.org/10.1016/j.saa.2012.09.068

Introduction

Cyclodextrins (CDs) are a family of cyclic oligosaccharides composed of α-(1,4) linked glucopyranose subunits. Cyclodextrins are useful molecular chelating agents. CDs possess a cage-like supramolecular structure, which let carry out chemical reactions that involve intramolecular interactions where covalent bonds are not formed between interacting molecules, ions or radicals [1]. In these complexes, a guest molecule is held within the lipophilic cavity of a cyclodextrin host molecule. The cyclodextrin cavity has an apolar character similar to an 80% dioxane/water solution and provides a slightly alkaline environment, because it is surrounded by glycosidic ethers. The main driving force of the complexation is the release of enthalpy-rich water molecules from the cavity [2–7]. Replacement of water molecules by more hydrophobic guest molecules present in the solution results in formation of an inclusion complex between the host and the guest [8]. This special ability to increase solubility, reduce bitterness, enhancing stability, and decreasing tissue irritation upon dosing. One of the most common applications of cyclodextrins cited in the pharmaceutical literature is the enhancement of bioavailability [9].

On the other hand, oxoisoaporphines are a family of isoquinoline alkaloids that have been isolated from the Menispermaceae and Sciadotenia toxifera families as the sole known natural sources present from Guatemala to Bolivia regions [10,11]. At the present, the chemical scaffold of oxoisoaporphine or 1-azabenzanthrone has been an interesting target due to pharmacological properties such as the inhibition of the human monoamino oxidase A (hMAO-A) and acetylcholinesterase (AChE) [12,13], antifungal activity [14] against human parasite [15], cytotoxicity against different tumor cell lines [16,17] and photo-electrochemical properties [18]. Since various years ago, our research group has developed extensive investigations about the nitro-compounds. The importance of nitro-heterocycle derivatives is focused in the existence of the withdrawing group able to obtain radicals species (ROS) affording oxidative stress, which is connected with some chemotherapies against *Trypanosoma cruzi* [19–23] in which synthetic drugs with nitro-containing heterocycles such as Nifurtimox® (Nfx) and Benznidazole® (Bnz) are used in clinic therapy. However, the chemotherapy is still inadequate due to its undesirable side effects, including cardiac and/or renal toxicity. Thus, these reasons justify the constant need for discovering and investigating new and effective agents against *Trypanosoma cruzi* (*T. cruzi*) [24]. In previous works [25,26] we verified that the incorporation of nitrocompounds in cyclodextrins improving its solubility and bioavailability. Furthermore, Maximiano et al. developed an effervescent tablets containing benznidazole complexed with cyclodextrin [27]. In this work, we give details about the synthesis, electrochemical characterization, spectroscopic and molecular modeling studies of a new nitro-oxoisoporphine derivative (ND). In the present study, we proposed the electrochemical mechanism and the inclusion model with β-cyclodextrin (βCD), hydroxypropyl-β-cyclodextrin (HPβCD) and 2,6-dimethyl-β-cyclodextrin (DMβCD) in order to increase the solubility of ND in aqueous medium and the modification of the its physico-chemistry properties for effects of the inclusion.

Experimental section

Reagents

The reagents β-cyclodextrin (βCD), heptakis(2,6-di-O-methyl)-β-cyclodextrin (DMβCD), 2-hydroxypropyl-β-cyclodextrin (HPβCD) and deuterated water (D_2O) were purchased from Sigma–Aldrich, Inc., St. Louis, MO. Other reagents were all analytical grade and double distilled water was used throughout.

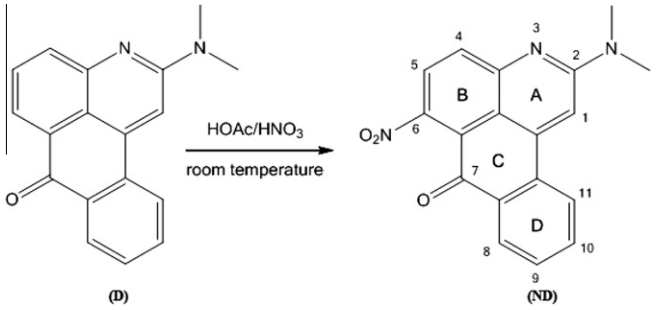

Scheme 1. Synthesis of **ND**.

Synthesis

The nitrooxoisoaporphine (**ND**)[1] derivative was synthesized according to following method (Scheme 1). To a stirred soln. of 2-(dimethylamino)-7*H*-naphtho [1,2,3-de]quinolin-7-one (**D**) (2.64 g, 9.63 mmol) in acetic acid (HOAc) (50 ml) was added dropwise fuming nitric acid (HNO_3) (3 ml) at room temperature during 1 h. Then, a yellow suspension was immediately formed. The formed precipitate yellow was filtered off and washed in water. The residue is recrystallized from acetonitrile (CH_3CN) to give 2.0 g (65%) of the respective 2-(dimethylamino)-6-nitro-7*H* naphtho[1,2,3-de]quinolin-7-one (**ND**) as brilliant yellow needles.

Cyclic voltammetry (CV) and Differential Pulse Polarography (DPP)

The CV and DPP measures were determinated in order to postulate an electrochemical mechanism and to know electrochemical response of ND in presence of β-CD, DMβCD and HPβCD, respectively. These experiments were performed in a Metrohm 693VA instrument with a 694VA Stand convertor and a 693VA Processor, under a nitrogen atmosphere at room temperature, by using a three electrode cell. A hanging mercury drop electrode (HMDE) was used as the working electrode, a platinum wire as the auxiliary electrode, and saturated calomel (SCE) as the reference electrode.

The CV experiment was carried out in dimethylformamide (DMF) with 0.1 M Tetrabutylammonium perchlorate (TBAP) as supporting electrolyte, being the final concentration of ND 1 mM. The DPP studies were realized in protic medium achieved in phosphate buffer (0.1 M ca. pH 7.4), the solutions were prepared starting from a stock solution 0.1 M of ND in DMSO. The final solution was prepared through the corresponding dilution to obtain a sample final concentration, on the voltammetric cell, of 1.0 mM. The cyclodextrin concentration was in the 0–3 mM range in electrochemical cell; finally 0.1 M KCl was used as supporting electrolyte.

ESR spectroscopy

ESR spectra were recorded in the X band (9.7 GHz) by using a Bruker ECS 106 spectrometer with a rectangular cavity and 50 kHz field modulation. The hyperfine splitting constants were estimated to be accurate within 0.05 G. The anion radicals were generated by electrolysis to controlled potential *in situ* by using DMSO as solvent and TBAP as supporting electrolyte. All experiments were carried out at room temperature and under nitrogen atmosphere. The concentration of ND used was 1 mM. The ESR

[1] Data of **ND**. M.p. > 300° (decomp.). IR (KBr): 1658 (C=O), 1384 (NO_2). ^{1}H NMR (400 MHz, tfa) δ 3.72 (s, 3H), 7.94 (t, *J* = 2.0 Hz, 1H), 8.03 (t, *J* = 2.0 Hz, 1H), 8.09 (t, *J* = 2.0 Hz, 1H), 8.19 (s, 1H), 8.24 (d, *J* = 1.0 Hz, 1H), 8.52 (d, *J* = 1.0 Hz, 1H), 8.61 (d, *J* = 1.0 Hz, 1H). ^{13}C NMR (400 MHz, tfa) δ 106.8, 110.1, 112.8, 115.7, 118.4, 123.8, 124.5, 127.3, 128.0, 129.0, 131.1, 131.4, 133.2, 133.4, 135.4, 141.6, 152.2, 185.0 CI–MS: 319 (M), 274 (MH^+). HR–CI–MS (MH—NO_2): 275.1184 ($C_{18}H_{15}N_2O$; calc. 275.1106).

spectra were simulated by using the program WINEPR Simphonia 1.25 version.

Phase-solubility measurements

Phase-solubility measurements were carried out according to the method of Higuchi and Connors [28], excess amount of ND (5 mg) was added to 5 ml of deionized water containing increasing amounts of βCD, HPβCD and DMβCD (ranging from 0 to 0.014 M). The resulting mixture was equilibrated in a Julabo thermostatic shaking water bath for 24 h at 30 °C after which the equilibrium was reached. The suspensions were filtered through 0.45 μm cellulose acetate membrane filter to remove undissolved solid. An aliquot from each vial was adequately diluted and spectrophotometrically analyzed at 358 nm (ε_{ND} = 9721 $M^{-1} * cm^{-1}$). The presence of β-cyclodextrin and their derivatives did not interfere in the spectrophotometric assay of ND–cyclodextrin complexes.

The apparent stability constant (Ka) of the complexes was calculated from the phase-solubility diagrams according to the following equation:

$$Ka = Slope/So\ (1 - Slope) \quad (1)$$

where So is the solubility of ND at 30 °C in the absence of cyclodextrin and slope means the corresponding slope of the phase-solubility diagrams, that is, the slope of the drug molar concentration versus CDs molar concentration graph.

NMR spectroscopy

One-dimensional ^{1}H NMR spectra were recorded at a probe temperature of 300 K on a Bruker DRX-500 operating at a proton NMR frequency of 500.13 MHz in unbuffered D_2O solutions. Acquisition parameters consisted of a spectral width of 5482 Hz, an acquisition time of 2.67 s and a relaxation delay of 1 s. 128 scans were recorded. FIDs were Fourier transformed with LB = 2.0 Hz and GB = 0. The resonance at 4.7 ppm due to residual solvent (HOD) was used as an internal reference.

Rotating-frame Overhauser effect spectroscopy (ROESY) spectra were acquired in the phase sensitive mode by using the same spectrometer and Bruker standard parameters. Each spectrum consisted of a matrix of 16 K (F2) by 8 K (F1) points covering a spectral width of 5482 Hz. Spectra were obtained from the samples solutions prepared for the ^{1}H NMR studies, by using a spin-lock mixing time of 400 ms, relaxation delay 2 s, and 32 scans were recorded.

Theoretical calculations

Full geometry optimizations of ND derivative as carried out with a conformational search by molecular mechanics (MMFF). Then, the most stable conformer was optimized by Becke's three parameter exact exchange functional, B3 [29] combined with gradient corrected correlation functional of Lee–Yang–Parr (LYP) [30] of the DFT method non-restricted basis using the 6-31G(d,p), which has proven to give acceptable results for organic radicals [31]. These calculations were followed by single-point runs on the optimized structures using UB3LYP/6-31*G. All calculations were performed with Gaussian 09 using DMSO as a solvent for the condensed phase under conductor-like polarizable continuum model (C-PCM) [32].

Molecular modeling

In silico build-up of DMβCD was carried out through the Builder module of the Insight II program [33] by adding to βCD 14 methyl in position 2 and 6 (DMβCD). The obtained models were subjected to optimization by using a protocol of 300 steps of conjugate gradients to avoid steric hindrance and clashes that can appear in the building process.

The ND was build with Gaussview and then it was optimized by using a semiempirical method such as AM1 [34,35] and then, optimized at the B3LYP/6-31G(d,p) level as implemented in Gaussian-09 package of programs [36]. ESP charges were obtained employing a single point at the B3LYP/6-31G* level as methodology of calculation [37]. Autodock 3.0.5 [38] with Lamarkian Genetic Algorithm (LGA) was used to generate the starting complexes. The parameters used for the global search was an initial population of 150 individuals, with a maximal number of energy evaluations of 15,000,000 and a maximal number of generations of 50,000 as end criterion. An elitism value of 1 was used, and a probability of mutation and crossing-over of 0.02 and 0.08 was used, respectively. From the best solutions obtained according to these parameters, some of them defined by the user as the best probabilities in our case 0.06 were further refined by a local search method such as pseudo Solis and Wets 'PSW'.

Autodock defines the conformational space implementing grids all over the space of the possible solutions. With the aim of testing the ability of Autodock to converge into solutions that are inside the DMβCD, a grid of 80 Å by the side and 0.3 Å spacing between each point was setup in such a way that it covered both the external surface and the internal cavity of the DMβCD.

The following procedure was employed on the DMβCD docking simulations: 200 runs were done. At the end of each run, the solutions were separated into clusters according to their lowest RMSD and the best score value based on a free empiric energy function. Cluster solutions whose average score was not over 1 kcal/mol with respect to the best energy obtained in the respective run were selected. Then, the solution that represents most of the complexes obtained in the run was compared with the NMR experimental data, assuring that this solution is able to represent it accurately.

Results and discussion

Cyclic voltammetry

Fig. 1a shows the voltammogram displayed by ND when DMSO solution of 1 mM of ND and 100 mM TBAP is swept from −0.3 to −2.0 V. We notice clearly a quasireversible couple (Ic/Ia) ($E_{1/2}$ = −0.46 V) for nitro anion radical generation from dicationic form (E_1). This indicates that the reduction could be more favorable in the biological medium, then a self-protonation process was proposed (C_1). In addition, according to Nicholson & Shain criteria, two reversible couples IIc/IIa and IIIc/IIIa were detected [39,40]. The redox couple IIc/IIa ($E_{1/2}$ = −1.10 V) corresponds to the nitro anion radical generation starting from the cationic form (E_2), this reduction potential was lower than Nifurtimox (−0.930 V) [41], Benznidazole (−1.019 V) [42] and Metronidazole (−1.160 V) [43]. Also, a second self-protonation process C_2 (peak II'c) was included. Finally, a new wave with a highest potential value (IIIc/IIIa, $E_{1/2}$ = −1.50 V was evidenced, and can be related to the carbonyl group reduction process E_3 [44].

$$(2H^+)—R—CO—NO_2 + e \rightarrow (2H^+)—R—CO—NO_2^{\cdot -} \quad (E1)$$

$$(2H^+)—R—CO—NO_2^{\cdot -} + (2H^+)—R—CO—NO_2 \rightarrow (2H^+)—R—CO—NO_2H^{\cdot} + H^+—R—CO—NO_2 \quad (C1)$$

$$H^+—R—CO—NO_2 + e \rightarrow H^+—R—CO—NO_2^{\cdot -} \quad (E2)$$

$$H^+—R—CO—NO_2^{\cdot -} + H^+—R—CO—NO_2 \rightarrow H^+—R—CO—NO_2H^{\cdot} + R—CO—NO_2 \quad (C2)$$

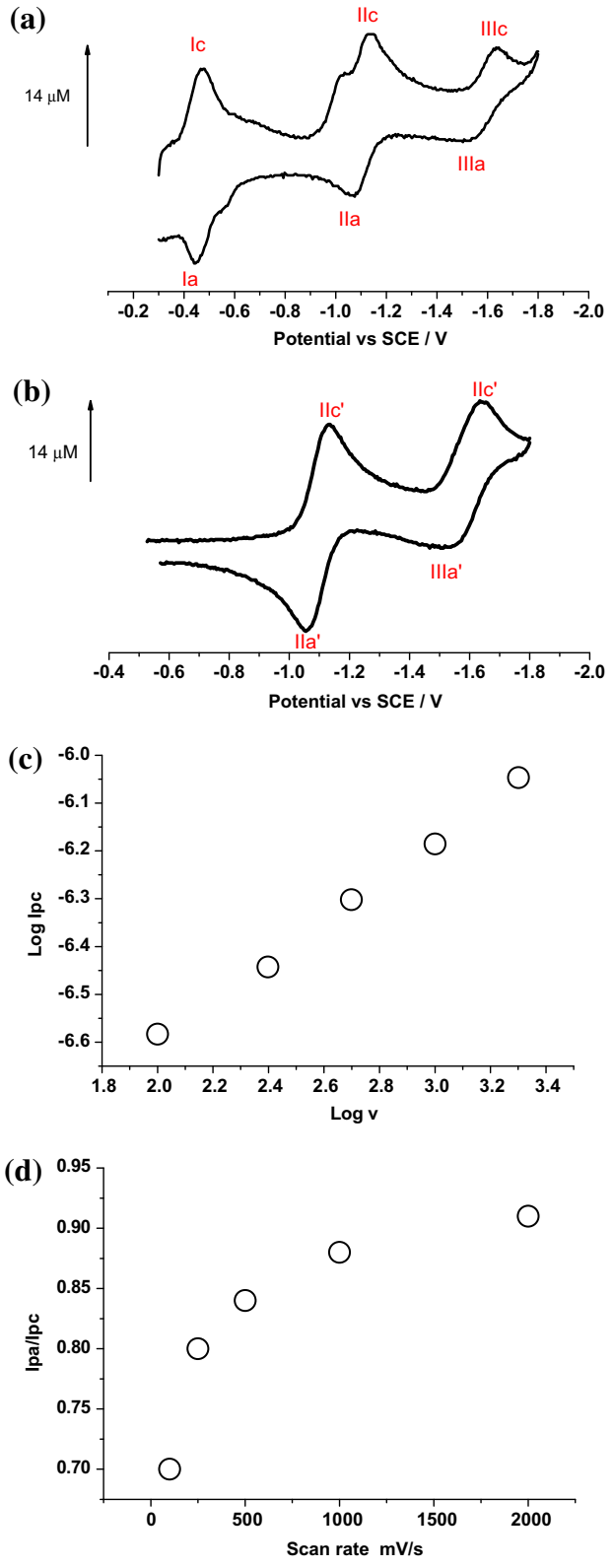

Fig. 1. (a) Cyclic voltammogram for ND derivative, (b) cyclic voltammogram in presence of NaOH, (c) diffusional control is represented by Log Ipc vs Log scan rate for IIc wave, and (d) graphic Ipa/Ipc vs scan rate for IIc wave.

$$R{-}CO{-}NO_2 + e \rightarrow R{-}CO^{\cdot -}{-}NO_2 \quad (E3)$$

In order to check the self-protonation mechanisms, the electrochemical experiments were carried out by applying increasing amounts of NaOH (0.1 M). Thus, the redox couples Ic and II'c were not evidenced, which confirm the presence of acid proton in the structure of ND and, therefore, the proposed self-protonation processes in this mechanism is confirmed. Thus, Fig. 1b shows the voltammetric response obtained for ND in neutral form, being observed only two redox couples corresponding to both the nitro and carbonyl group reduction, respectively.

In this conditions, we measure to different scan rate (100–2000 mV/s range) that allow corroborate the reversibility of the redox couple II as well the diffusional control of this reduction (Fig. 1c and d).

ESR Spectroscopy

The electrochemical reduction (*in situ*) of ND free radical in DMSO was carried out by applying the potential corresponding to the first wave from cyclic voltammetry experiments (Fig. 2). The interpretation of the ESR spectrum was done in terms of their experimental hyperfine coupling constants for each magnetic center. The ESR simulated spectrum which reached the best agreement with the experimental one (Fig. 2) suggests a hyperfine splitting pattern composed by one triplet corresponding to N(from NO_2 group, aN = 3.805 Gauss) and five doublets (aH_v = 3.730 Gauss, aH_w = 2.660 Gaus, aH_x = 1.549 Gauss, aH_y = 1.440 Gauss, aH_z = 0.658 Gauss). On the other hand, theoretical calculations confirm the observed experimental patterns allowing us to confirm the triplet of N(from NO_2 group, $aN_{theoretical}$ = 3.153 Gauss) but also assign the doublets corresponding to the hydrogens H-4, -1, -$N(CH_3)_2$, -10 and -5 with theoretical hyperfine constants around $aH_{v=H-4}$ = 3.220 Gauss, $aH_{w=H-1}$ = 3.174 Gaus, $aH_{x=N(CH3)2}$ = 1.555 Gauss, $aH_{y=H-10}$ = 1.174 Gauss and $aH_{z=H-5}$ = 1.113 Gauss respectively. Thus, theoretical calculations have shown a good theoretical/experimental agreement besides a high accuracy and suitability for this kind of estimation. Moreover, these findings indicate that the unpaired electron is located over the entire molecule as a whole, even reaching the R–$N(CH_3)_2$ group likely due to resonance effects as shown in Fig. 3. Consequently, a highly delocalized system is reached by ND free radical, where, even when the ND free radical generation takes place over the NO_2 group as reduction center, the high delocalization throughout the molecule produces an ESR spectrum comparable to that observed for

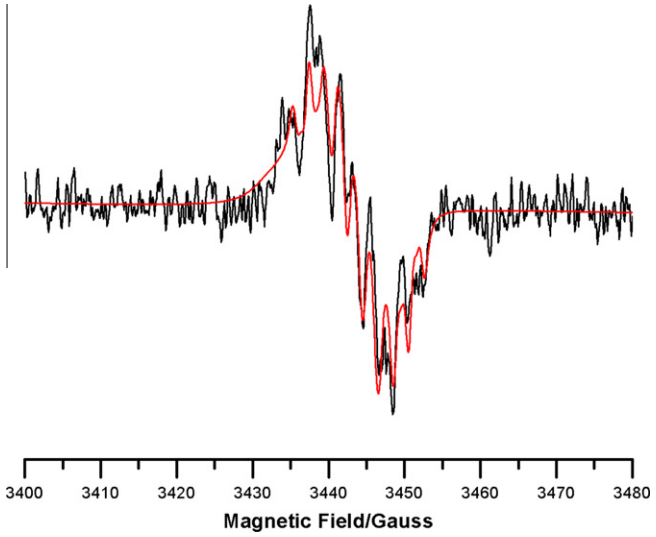

Fig. 2. Experimental (black) and simulated (red) ESR spectra for ND free radical. Spectrometer conditions: Microwave frequency, 9.68 GHz; microwave power, 20 mW; amplitude modulation, 0.20 G; time constant, 81.92 mS. Linewidth: 0.744; g_{value}, 2.011Gauss. (For interpretation of the references to color in this figure legend, the reader is referred to the web version of this article.)

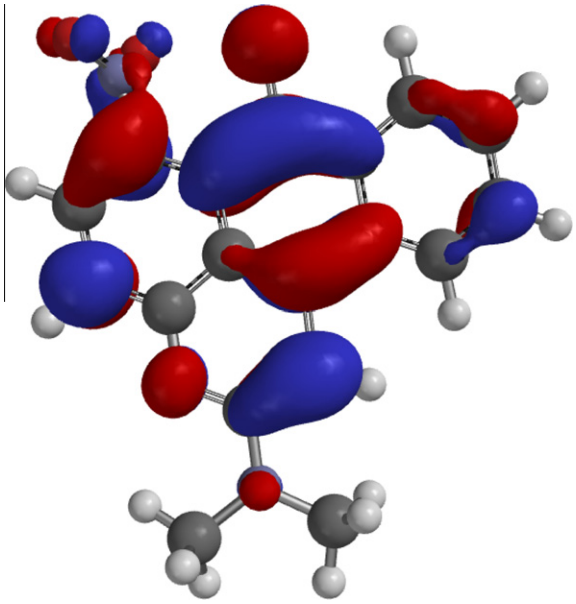

Fig. 3. Single occupied molecular orbital (SOMO) for ND free radical. Optimization geometries procedures converge in a structure for ND with the NO_2 group out of the molecule plane. This particular geometry does not allow that the unpaired electron is located just over the B ring (likely because the moiety lacks of a significant resonance between NO_2 group and B ring) when the reduction process takes place. However, the resonant phenomena's between A, B and C rings produce that the unpaired electron is mainly placed over the CO group but highly delocalized throughout the molecule, in agree with the ESR spectrum for ND, similar to that expected for a CO group instead of a NO_2.

carbonyl derivatives as described earlier for 5-nitroindazoles [45,46] or Naphtoquinones [47,48] derivatives instead of showing the typical ESR spectrum exhibited by NO_2 derivatives.

Phase-solubility measurements

These experiments were realized in order to improve aqueous solubility of ND by ND-β-CDs complexes formation. Fig. 4a shows an absorption spectra for ND-DMβCD complex, where an increment in absorbance units is observed when cyclodextrin is added to the system, being this behavior evidenced for all complexes formed.

These results allow to afford a [ND] vs [CD] plot (Fig. 4b), and through a linear fitting treatment (from Eq. (1)), The shape of all the solubility diagrams followed an A_L-type system [28], where a linear increase of ND solubility was observed as function of CDs concentration, over the entire concentration. This linear host–guest correlation spectroscopy with slope of less than 1 suggested the formation of first order soluble complexes with respect to CD concentration [49]. Association constant values (Ka) for all the complexes ND-CD were obtained. Complex ND-βCD evidenced a Ka value of $125 \pm 6\ M^{-1}$. On the contrary, ND-DMβCD and ND-HPβCD complexes, these showed an increment in the Ka values of $2021 \pm 16\ M^{-1}$ and $4154 \pm 12\ M^{-1}$ respectively. The higher Ka values for ND-DMβCD and ND-HPβCD indicate the different abilities to form inclusion complexes between ND with β-CD and its derivatives. The derivatization of β-cyclodextrin cavity, increase mainly the size allowing a better complexation process for this kind of alkaloids. The fact implies that the cavity of modified CD provides a better protective microenvironment. This is probably because the hydroxypropyl substitutions that enlarge the opening of native β-CD and destroy the strong intramolecular hydrogen bond network, which lets guest molecules access into the HP-CD cavity easily and give a higher stability constant [50].

Differential Pulse Polarography (DPP)

DPP was used in order to assess the effect of the reduction potential and cathodic current by complexes formation between ND and β-cyclodextrin, 2,6-dymethyl-β-cyclodextrin, and 2-hydroxypropyl-β-cyclodextrin. Fig. 5 shows the different electrochemical behaviors of ND at different concentrations of cyclodextrin in the system, which are dependent of Ka values.

Thus, a decreasing of the cathodic current is observed when CD is added to the system (with respect to the free ND), which reveals a modification in the transport phenomena from the solution toward the interface electrode-solution governed by diffusional processes. This low effect is produced by the complexes formation. Also, the reduction potential is displaced toward longer potential depending of Ka values. For ND-βCD this variation is not observed ($Ka = 125 \pm 6\ M^{-1}$). In the case of ND-DMβCD ($Ka = (2021 \pm 16\ M^{-1}$) and ND-HPβCD ($Ka = 4254 \pm 12\ M^{-1}$) a shift to higher reduction potential is observed, presumably when the nitro group is incorporated inside the cyclodextrin cavity, which is corroborated by 2D NMR techniques.

NMR spectroscopy

The inclusion geometry of ND-DMβCD complex was determinated by using NMR experiments. The protons of ND showed fre-

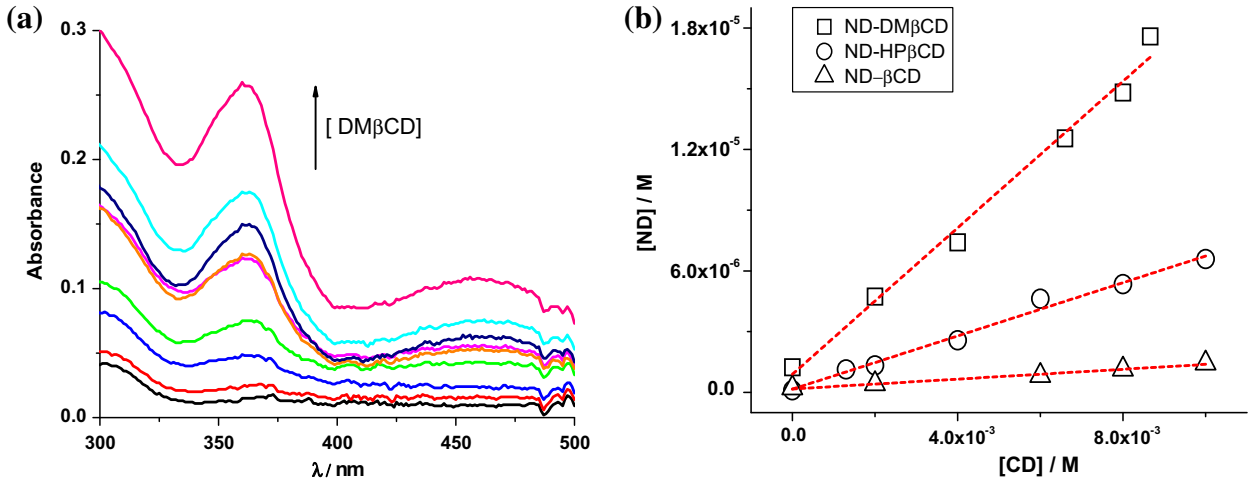

Fig. 4. (a) Absorption spectra for ND-DMβCD complex and (b) graphic [ND] vs [CD].

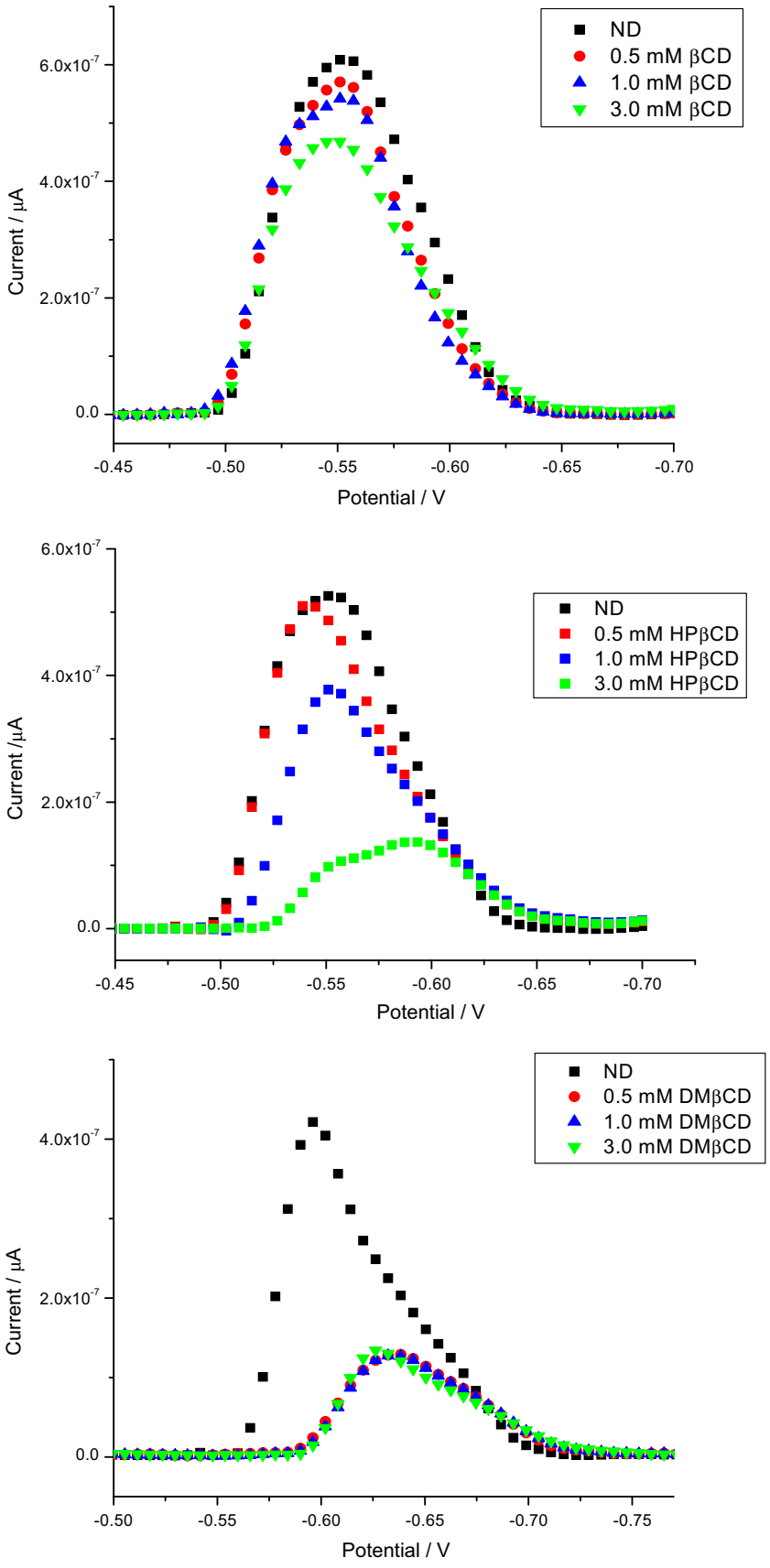

Fig. 5. Differential Pulse Polarography for ND in presence of different concentrations of β-cyclodextrins.

Table 1
^{1}H NMR shifts (δ) multiplicity (m) for **2** in the absence and presence of DMβCD ($\Delta\delta$ = δfree- bound) in D_2O.

	m	δ_{free}	δ_{bound}	$\Delta\delta$
ND proton				
H-1	s	6.80	6.89	−0.09
H-4	m	7.67	7.67	0
H-5	m	7.69	7.68	0.01
H-8	m	7.40	7.58	−0.18
H-9	m	7.43	7.59	−0.16
H-10	m	7.46	7.60	−0.14
H-11	m	7.67	7.87	−0.20
CD proton				
H-3		3.85	3.81	0.04
H-5		3.77	3.74	0.03
H-6		3.61	3.62	−0.01
H-4		3.50	3.50	0
H-2		3.23	3.27	−0.04

quency changes in presence of DMβCD (Table 1). The induced shift $\Delta\delta$ is defined as the difference in chemical shift in the absence and presence of the other reactants.

Thus, the induced shifts were calculated by the following equation: $\Delta\delta$ = δfree − δbound. In this sense, the negative and positive signs show low and high frequency shifts, respectively. Downfield shifts are observed for the aromatic protons in D ring. However, the major induced deshielding is observed from H-8 to H-11, being this last one the most affected. The movements of these proton signals suggested that the penetration of this compound involves insertion of the D ring portion inside the cavity. This interpretation is supported by upfield displacement mainly of the H-3 proton, and in minor intensity of the H-5 proton of the annular interior of DMβCD. This displacement is due to the anisotropic magnetic effect induced by the presence of the aromatic group of the guest molecule. Due to the H-6 proton of the CD is not affected by the aromatic ring, we can concluded that the insertion of the compound is through the wider rim, affording a complex where the other aromatic rings are not involved (Fig. 6).

Molecular modeling

In order to rationalize the experimental NMR results, molecular modeling studies on the ND-DMβCD complex were done. The theoretical interaction mode for ND-DMβCD inclusion complex is shown in Fig. 7. It is noteworthy to note that though no fixed distances were imposed during the docking calculations, the results are in agreement with that obtained by the 2D ROESY spectra.

Molecular modeling results suggest a preferred final relative orientation for this complex, where the heterocycle is inserted in the DMβCD cavity with the nitro and dimethylamine groups oriented to the secondary rim. However, the nitro group is partially positioned within the cavity whilst the dimethylamine group is exposed to the outside (Fig. 7a).

Conformationally, the heterocycle is sited in a slight inclination regarding the glycosidic oxygen plane. This orientation makes the D-ring interacts with H-3′ and H-5′, which confirms the peaks corresponding to H-8/H-9/H-10. In addition, as shown in Fig. 7b, the heterocycle is positioned in such way that H-11 is near to H-3′ but far from H-5′, which is confirmed by the 2D ROESY spectrum. As mentioned, the B-ring is partially exposed to the outside. However, the relative inclination of the ring allows the interaction between H-4 and H-5 with H-3′. Finally, H-1(from A-ring) interacts strongly with the 2-methyl group from DMβCD likely due to the partial exposition of the A ring.

Thus, molecular modeling results give us a three-dimensional space perspective about the inclusion complex of ND with DMβCD, in complete agreement with 2D NMR ROESY experiments. In this

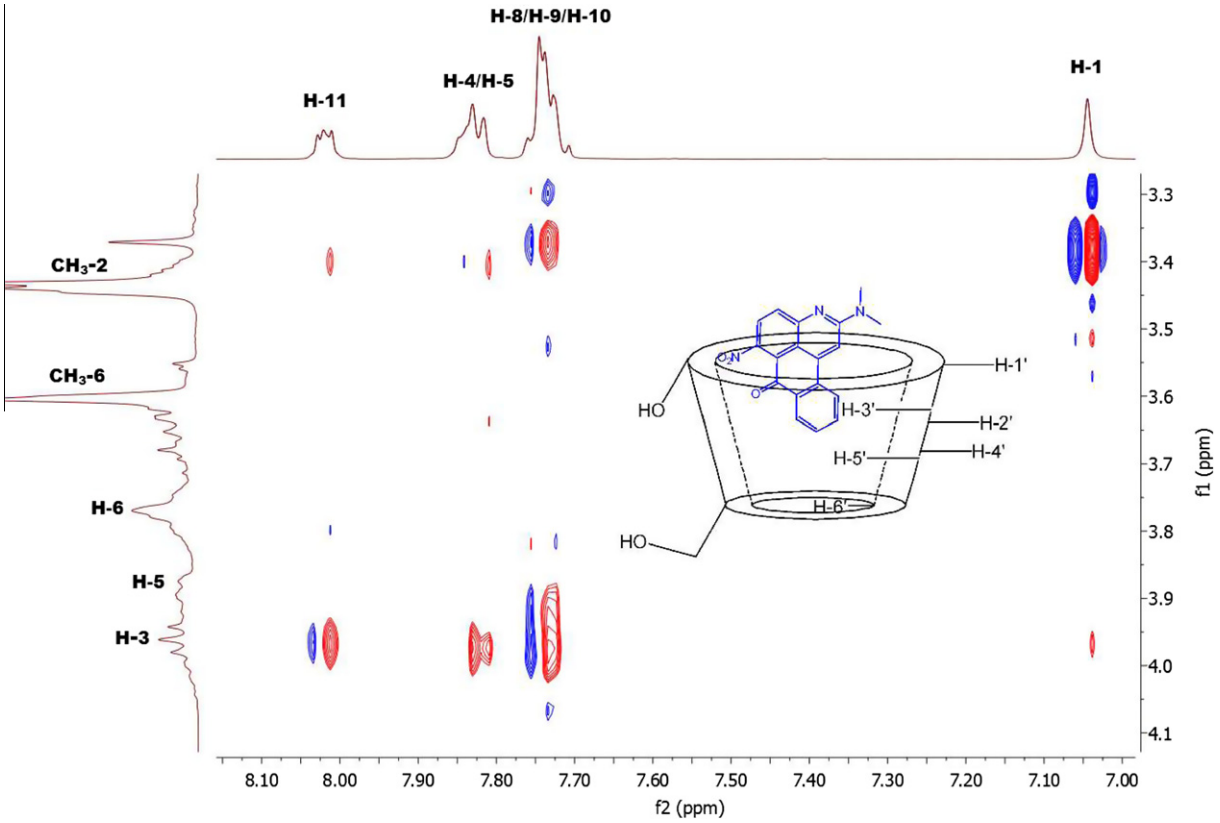

Fig. 6. Partial contour plot of the two-dimensional ROESY spectrum of **ND** in the presence of DMβCD in D_2O.

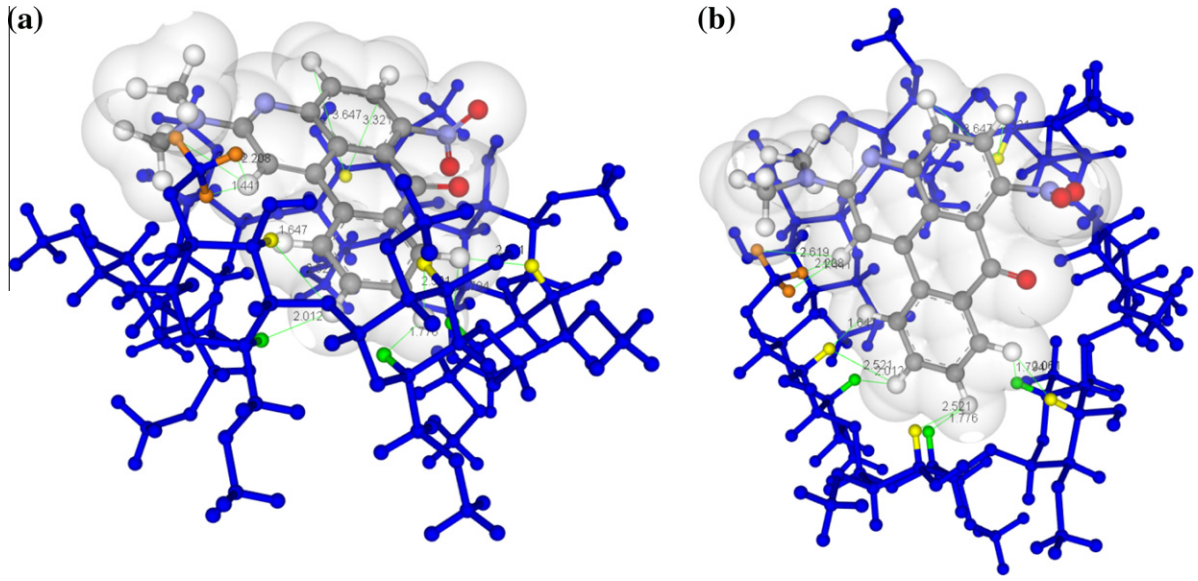

Fig. 7. Interaction mode for ND-DMβCD obtained from molecular docking studies. The C- and D-rings are almost completely inserted on the interior of the CD, whilst the A and -B -rings are partially exposed to the outside. Interacting H-3′, H-5′ and 2-CH_3 (from DMβCD) are denoted by the yellow, green and brown colors respectivly from (a) frontal and (b) secundary rim perspective. (For interpretation of the references to color in this figure legend, the reader is referred to the web version of this article.)

sense, the partial protection of the nitro group by the DMβCD cavity has also been confirmed, which also in agreement by our electrochemical results.

Conclusions

The aqueous solubility of ND has been improved in neutral aqueous solutions through complexation with β-cyclodextrins. These results indicated the interaction between ND and cyclodextrin derivatives in water forming 1:1 inclusion complex. The stability constant of the inclusion complex is measured as 125 M^{-1}, 4154 M^{-1}, 2021 M^{-1} for βCD, HPβCD and DMβCD, respectively.

The effect of βCDs on the polarographic behavior of ND can be summarized in a negative shift in the cathodic peak potential for HPβCD and DMβCD in addition a peak current decrease. However, in the complex ND-βCD only a small change in the IPC can be observed. From these changes we can assume that the nitroaromatic group in the DMβCD and HPβCD is more hindered.

By means of experimental and theoretical methods, the present work unambiguously determined the geometrical inclusion parameters of ND-DMβCD, showing that the 2D ROESY experiments confirm the inclusion of ND in DMβCD. These results were corroborated by molecular modeling calculations, as well.

Acknowledgements

Fernanda Pérez-Cruz gratefully acknowledges CONICYT-Chile for Doctoral fellowship, fellowship for doctoral theses support CONICYT-Chile No. 24110059, Mecesup fellowship – Mecesup project UCH-0601, Becas-Chile and Fulbright Fellowships for Doctoral Stay. Benjamin Aguilera-Venegas thanks financials support by FONDECYT Grants No. 3130364, E. Sobarzo-Sánchez thanks to "Isidro Parga Pondal" Program for financial support.

References

[1] E.M.M. Del Valle, Cyclodextrins and their uses: a review, Process Biochemistry 39 (2004) 1033–1046.
[2] R.L. Carrier, L.A. Miller, I. Ahmed, The utility of cyclodextrins for enhancing oral bioavailability, Journal of Controlled Release 123 (2007) 78–99.
[3] J. Szejtli, Introduction and general overview of cyclodextrin chemistry, ChemInform 29 (1998) 1743–1754.
[4] J. Szejtli, Medicinal applications of cyclodextrins, Medicinal Research Reviews 14 (1994) 353–386.
[5] C. Jullian, S. Miranda, G. Zapata-Torres, F. Mendizábal, C. Olea-Azar, Studies of inclusion complexes of natural and modified cyclodextrin with (+)catechin by NMR and molecular modeling, Bioorganic and Medicinal Chemistry 15 (2007) 3217–3224.
[6] H.A. Archontaki, M.V. Vertzoni, M.H. Athanassiou-Malaki, Study on the inclusion complexes of bromazepam with β- and β-hydroxypropyl-cyclodextrins, Journal of Pharmaceutical and Biomedical Analysis 28 (2002) 761–769.
[7] I.V. Terekhova, Comparative thermodynamic study on complex formation of native and hydroxypropylated cyclodextrins with benzoic acid, Thermochimica Acta 526 (2011) 118–121.
[8] S. Brochsztain, M.A. Rodrigues, M.J. Politi, Inclusion complexes of naphthalimide derivatives with cyclodextrins, Journal of Photochemistry and Photobiology A: Chemistry 107 (1997) 195–200.
[9] C. Folch-Cano, C. Jullian, H. Speisky, C. Olea-Azar, Antioxidant activity of inclusion complexes of tea catechins with β-cyclodextrins by ORAC assays, Food Research International 43 (2010) 2039–2044.
[10] L. Killmer, F.G. Vogt, A.J. Freyer, M.D. Menachery, C.M. Adelman, Lakshminine, a new rare oxoisoaporphine alkaloid from Sciadotenia toxifera, and structural revisions of telazoline and teladiazoline, two related oxoaporphines from *Telitoxicum peruvianum* and *T. glaziovii*, Journal of Natural Products 66 (2002) 115–118.
[11] Y. Sugimoto, H.A.A. Babiker, S. Inanaga, M. Kato, A. Isogai, Oxoisoaporphines from *Menispermum dauricum*, Phytochemistry 52 (1999) 1431–1435.
[12] H. Tang, F.-X. Ning, Y.-B. Wei, S.-L. Huang, Z.-S. Huang, A.S.-C. Chan, L.-Q. Gu, Derivatives of oxoisoaporphine alkaloids: a novel class of selective acetylcholinesterase inhibitors, Bioorganic and Medicinal Chemistry Letters 17 (2007) 3765–3768.
[13] H. Tang, X.-D. Wang, Y.-B. Wei, S.-L. Huang, Z.-S. Huang, J.-H. Tan, L.-K. An, J.-Y. Wu, A. Sun-Chi Chan, L.-Q. Gu, Oxoisoaporphine alkaloid derivatives: synthesis, DNA binding affinity and cytotoxicity, European Journal of Medicinal Chemistry 43 (2008) 973–980.
[14] Y.-P. Li, F.-X. Ning, M.-B. Yang, Y.-C. Li, M.-H. Nie, T.-M. Ou, J.-H. Tan, S.-L. Huang, D. Li, L.-Q. Gu, Z.-S. Huang, Syntheses and characterization of novel oxoisoaporphine derivatives as dual inhibitors for cholinesterases and amyloid beta aggregation, European Journal of Medicinal Chemistry 46 (2011) 1572–1581.
[15] H. González-Díaz, F. Prado-Prado, E. Sobarzo-Sánchez, M. Haddad, S. Maurel Chevalley, A. Valentin, J. Quetin-Leclercq, M.A. Dea-Ayuela, M. Teresa Gomez-Muños, C.R. Munteanu, J. José Torres-Labandeira, X. García-Mera, R.A. Tapia, F.M. Ubeira, NL MIND-BEST: a web server for ligands and proteins discovery – theoretic-experimental study of proteins of *Giardia lamblia* and new compounds active against *Plasmodium falciparum*, Journal of Theoretical Biology 276 (2011) 229–249.
[16] F. Prado-Prado, X. García-Mera, M. Escobar, E. Sobarzo-Sánchez, M. Yañez, P. Riera-Fernandez, H. González-Díaz, 2D MI-DRAGON: a new predictor for protein–ligands interactions and theoretic-experimental studies of US FDA drug-target network, oxoisoaporphine inhibitors for MAO-A and human

parasite proteins, European Journal of Medicinal Chemistry 46 (2011) 5838–5851.
[17] V. Castro-Castillo, M. Rebolledo-Fuentes, C. Theoduloz, B.K. Cassels, Synthesis of lakshminine and antiproliferative testing of related oxoisoaporphines, Journal of Natural Products 73 (2010) 1951–1953.
[18] C. Aliaga, M. Cerón-Neculpán, C. Saitz, C. Jullian, E. Sobarzo-Sánchez, J.R. De la Fuente, Oxoisoaporphines: regioselective deuterium labelling involving the metastable hydrogenated photoproduct anions, Journal of Photochemistry and Photobiology A: Chemistry 222 (2011) 360–365.
[19] G. Aguirre, E. Cabrera, H. Cerecetto, R. Di Maio, M. González, G. Seoane, A. Duffaut, A. Denicola, M.J. Gil, V. Martínez-Merino, Design, synthesis and biological evaluation of new potent 5-nitrofuryl derivatives as anti-*Trypanosoma cruzi* agents. Studies of trypanothione binding site of trypanothione reductase as target for rational design, European Journal of Medicinal Chemistry 39 (2004) 421–431.
[20] G. Barriga, C. Olea-Azar, E. Norambuena, A. Castro, W. Porcal, A. Gerpe, M. González, H. Cerecetto, New heteroaryl nitrones with spin trap properties: Identification of a 4-furoxanyl derivative with excellent properties to be used in biological systems, Bioorganic and Medicinal Chemistry 18 (2010) 795–802.
[21] C. Olea-Azar, H. Cerecetto, A. Gerpe, M. González, V.J. Arán, C. Rigol, L. Opazo, ESR and electrochemical study of 5-nitroindazole derivatives with antiprotozoal activity, Spectrochimica Acta Part A: Molecular and Biomolecular Spectroscopy 63 (2006) 36–42.
[22] L. Otero, G. Aguirre, L. Boiani, A. Denicola, C. Rigol, C. Olea-Azar, J.D. Maya, A. Morello, M. González, D. Gambino, H. Cerecetto, Nitrofurylsemicarbazone rhenium and ruthenium complexes as anti-trypanosomal agents, European Journal of Medicinal Chemistry 41 (2006) 1231–1239.
[23] J. Rodríguez, C. Olea-Azar, G. Barriga, C. Folch, A. Gerpe, H. Cerecetto, M. González, Comparative spectroscopic and electrochemical study of nitroindazoles: 3-alcoxy, 3-hydroxy and 3-oxo derivatives, Spectrochimica Acta Part A: Molecular and Biomolecular Spectroscopy 70 (2008) 557–563.
[24] C. Maria Aravena, A. Claudio Olea, H. Cerecetto, M. González, J.D. Maya, J. Rodríguez-Becerra, Potent 5-nitrofuran derivatives inhibitors of *Trypanosoma cruzi* growth: electrochemical, spectroscopic and biological studies, Spectrochimica Acta Part A: Molecular and Biomolecular Spectroscopy 79 (2011) 312–319.
[25] C. Jullian, J. Morales-Montecinos, G. Zapata-Torres, B. Aguilera, J. Rodriguez, V. Arán, C. Olea-Azar, Characterization, phase-solubility, and molecular modeling of inclusion complex of 5-nitroindazole derivative with cyclodextrins, Bioorganic & Medicinal Chemistry 16 (2008) 5078–5084.
[26] F. Pérez-Cruz, C. Jullian, J. Rodriguez, V.J. Arán, C. Olea-Azar, Molecular encapsulation of 5-nitroindazole derivatives in 2,6-dimethyl-[beta]-cyclodextrin: electrochemical and spectroscopic studies, Bioorganic & Medicinal Chemistry 17 (2009) 4604–4611.
[27] F.P. Maximiano, G.H.Y. Costa, L.C.L. de Sá Barreto, M.T. Bahia, M.S.S. Cunha-Filho, Development of effervescent tablets containing benznidazole complexed with cyclodextrin, Journal of Pharmacy and Pharmacology 63 (2011) 786–793.
[28] T. Higuchi, K.A. Connors, Phase-solubility techniques, Advances in Analytical Chemistry and Instrumentation 4 (1965) 117.
[29] A.D. Becke, Density-functional exchange-energy approximation with correct asymptotic-behavior, Physical Review A 38 (1988) 3098–3100.
[30] C.T. Lee, W.T. Yang, R.G. Parr, Development of the colle-salvetti correlation-energy formula into a functional of the electron-density, Physical Review B 37 (1988) 785–789.
[31] L. Hermosilla, P. Calle, J.M.G. de la Vega, C. Sieiro, Density functional theory study of N-14 isotropic hyperfine coupling constants of organic radicals, Journal of Physical Chemistry A 110 (2006) 13600–13608.
[32] V. Barone, M. Cossi, Quantum calculation of molecular energies and energy gradients in solution by a conductor solvent model, Journal of Physical Chemistry A 102 (1998) 1995–2001.
[33] Insight II, MSI, San Diego, California.
[34] C. Alemán, M.C. Vega, J.J. Perez, On the reliability of MINDO/3, MNDO and AM1 radical geometries for the computation of INDO electron spin resonance hyperfine coupling constants, Journal of Molecular Structure: THEOCHEM 281 (1993) 39–44.
[35] M.J.S. Dewar, E.G. Zoebisch, E.F. Healy, J.J.P. Stewart, Development and use of quantum mechanical molecular models. 76. AM1: a new general purpose quantum mechanical molecular model, Journal of the American Chemical Society 107 (1985) 3902–3909.
[36] G.W.T. M.J. Frisch, H.B. Schlegel, G.E. Scuseria, J.R.C.M.A. Robb, G. Scalmani, V. Barone, B. Mennucci, H.N.G.A. Petersson, M. Caricato, X. Li, H.P. Hratchian, J.B.A.F. Izmaylov, G. Zheng, J.L. Sonnenberg, M. Hada, K.T.M. Ehara, R. Fukuda, J. Hasegawa, M. Ishida, T. Nakajima, O.K.Y. Honda, H. Nakai, T. Vreven, J.A. Montgomery Jr., F.O.J.E. Peralta, M. Bearpark, J.J. Heyd, E. Brothers, V.N.S.K.N. Kudin, R. Kobayashi, J. Normand, A.R.K. Raghavachari, J.C. Burant, S.S. Iyengar, J. Tomasi, N.R.M. Cossi, J.M. Millam, M. Klene, J.E. Knox, J. B. Cross, C.A.V. Bakken, J. Jaramillo, R. Gomperts, R. E. Stratmann, A.J.A.O. Yazyev, R. Cammi, C. Pomelli, J.W. Ochterski, K.M.R.L. Martin, V.G. Zakrzewski, G.A. Voth, J.J.D.P. Salvador, S. Dapprich, A.D. Daniels, J.B.F.O. Farkas, J.V. Ortiz, J. Cioslowski, G.D.J. Fox, Inc., Wallingford CT, 2009., Gaussian 09, Revision A.02, 2009.
[37] B. Aguilera-Venegas, C. Olea-Azar, E. Norambuena, V.J. Arán, F. Mendizábal, M. Lapier, J.D. Maya, U. Kemmerling, R. López-Muñoz, ESR, electrochemical, molecular modeling and biological evaluation of 4-substituted and 1,4-disubstituted 7-nitroquinoxalin-2-ones as potential anti-*Trypanosoma cruzi* agents, Spectrochimica Acta Part A: Molecular and Biomolecular Spectroscopy 78 (2011) 1004–1012.
[38] G.M. Morris, D.S. Goodsell, R.S. Halliday, R. Huey, W.E. Hart, R.K. Belew, A.J. Olson, Automated docking using a Lamarckian genetic algorithm and an empirical binding free energy function, Journal of Computational Chemistry 19 (1998) 1639–1662.
[39] R.S. Nicholson, Semiempirical procedure for measuring with stationary electrode polarography rates of chemical reactions involving the product of electron transfer, Analytical Chemistry 38 (1966) 1406.
[40] R.S. Nicholson, I. Shain, Theory of stationary electrode polarography. Single scan and cyclic methods applied to reversible, irreversible, and kinetic systems, Analytical Chemistry 36 (1964) 706–723.
[41] C. Folch-Cano, C. Olea-Azar, V.J. Arán, C. Diaz-Urrutia, ESR and electrochemical study of 1,2-disubstituted 5-nitroindazolin-3-ones and 2-substituted 3-alkoxy-5-nitro-2H-indazoles: reactivity and free radical production capacity in the presence of biological systems, Spectrochimica Acta Part A: Molecular and Biomolecular Spectroscopy 75 (2010) 375–380.
[42] P.J.S. Barbeira, G.M. Silva, M.d.L.P.M. Beatriz, N.R. Stradiotto, Polarographic determination of benznidazole in DMSO, Journal of Pharmaceutical and Biomedical Analysis 20 (1999) 723–726.
[43] S. Bollo, L.J. Núñez-Vergara, J.A. Squella, Cyclic voltammetric determination of free radical species from nitroimidazopyran: a new antituberculosis agent, Journal of Electroanalytical Chemistry 562 (2004) 9–14.
[44] C. Olea-Azar, B. Abarca, E. Norambuena, L. Opazo, C. Rigol, R. Ballesteros, M. Chadlaoui, ESR and electrochemical studies of 2-acylpyridines and 6,6′-diacyl-2,2′-bipyridines, Spectrochimica Acta Part A: Molecular and Biomolecular Spectroscopy 61 (2005) 2261–2266.
[45] B. Aguilera-Venegas, C. Olea-Azar, V.J. Arán, J.D. Maya, U. Kemmerling, H. Speisky, F. Mendizábal, Electrochemical, ESR and theoretical insights into the free radical generation by 1,1′-hydrocarbylenebisindazoles and Its evaluation as potential bio-active compounds, International Journal of Electrochemical Science 7 (2012) 5837–5863.
[46] C.A. Díaz-Urrutia, C.A. Olea-Azar, G.A. Zapata, M. Lapier, F. Mura, B. Aguilera-Venegas, V.J. Arán, R.A. López-Múñoz, J.D. Maya, Biological and chemical study of fused tri- and tetracyclic indazoles and analogues with important antiparasitic activity, Spectrochimica Acta Part A: Molecular and Biomolecular Spectroscopy 95 (2012) 670–678.
[47] C.d.O. Costa, E.d.O. Costa, F.d.R. Ferreira, L.d.S. Viana, L.V.d. Silva, F.d.A.d.S. Silva, F.C.d. Abreu, I.M. Figueiredo, W.P. Jr., E.d.S. Bento, T.L.G. Lemos, O.D.L. Pessoa, B. Aguilera-Venegas, E. Norambuena, C. Olea-Azar, M.O.F. Goulart, Oncocalyxone A: Electrochemical, Spectroscopic Investigation and Studies of Its Interaction with DNA, Nucleobases and N-Acetylcysteine, Journal of the Brazilian Chemical Society 23 (2012) 1174–1185.
[48] E.d.O. Costa, M.T. Molina, F.C.d. Abreu, F.d.A.d.S. Silva, C.d.O. Costa, W.P. Jr., B. Valentim, B. Aguilera-Venegas, F. Pérez-Cruz, E. Norambuena, C. Olea-Azar, M.O.F. Goulart, Electrochemical and spectroscopic investigation of bioactive naphthoquinones, International Journal of Electrochemical Science 7 (2012) 6524–6538.
[49] C.M. Fernandes, M. Teresa Vieira, F.J.B. Veiga, Physicochemical characterization and in vitro dissolution behavior of nicardipine–cyclodextrins inclusion compounds, European Journal of Pharmaceutical Sciences 15 (2002) 79–88.
[50] Z. Lu, B. Cheng, Y. Hu, Y. Zhang, G. Zou, Complexation of resveratrol with cyclodextrins: Solubility and antioxidant activity, Food Chemistry 113 (2009) 17–20.